JOURNAL OF MATERIALS SCIENCE 19 (1984) 552–566

X-ray orientation and hardness experiments on RDX explosive crystals

W. L. ELBAN, J. C. HOFFSOMMER
Naval Surface Weapons Center, Silver Spring, Maryland 20910, USA

R. W. ARMSTRONG*
University of Maryland, College Park, Maryland 20742, USA

RDX (cyclotrimethylenetrinitramine) explosive crystals, typically approaching 5 mm in size, were grown by evaporation from acetone solution using production-grade crystals as starting material. Two distinctly different morphologies resulted, including one that apparently has not been previously reported in other investigations. These morphologies were characterized using Laue X-ray diffraction methods and an optical trace analysis, both involving a stereographic projection description. Microindentation experiments were performed on different prominent growth surfaces of several selected laboratory-grown crystals having the conventional morphology type. The hardness results are compared with measurements made directly on several production-grade crystals having a different morphology, and are compared with preceding measurements on a crystal having the previously unreported morphology. The latter crystal exhibited highly localized plastic deformation at the indentations as revealed by dislocation etch-pitting. Observations are made regarding the dislocation structure and cleavage properties of RDX based on its orthorhombic unit cell.

1. Introduction

Investigating the localized nature of plastic deformation processes in explosive crystals is important in understanding initiation processes in these materials when they are subjected to mechanical forces [1–3]. Individual production-grade explosive crystals are small in size (Fig. 1). Larger crystals, with about the same chemical composition as production-grade crystals so that any impurity effect will not be significantly altered, are more amenable to analysis. However, in studying the deformation behaviour of large explosive crystals so as to understand the sequence of events culminating in detonation in production materials having considerably smaller particles sizes, it is important to be aware of the well-established observation [4, 5] that explosives are known to be much more sensitive, at least in terms of their shock-to-detonation threshold, when in the form of powders.

Currently, an effort [6] is underway to determine the degree and nature of localized plastic deformation behaviour of RDX (cyclotrimethylenetrinitramine), a molecular crystalline explosive ingredient widely used in munitions. This study is connected with the proposal [7] that the generation of "hot spots" within deforming materials, including crystalline explosives such as RDX, comes from the obstruction of dislocation pile-ups by strong internal obstacles which collapse suddenly to give adiabatic dissipation of the very localized interaction energy stored by the bunched-up dislocations. The dislocation self-energies are negligible by comparison.

In order to investigate the local deformation properties of RDX crystals in a controlled way, microindentation hardness experiments have been performed on various prominent growth facets using Knoop and Vickers indenters. The Knoop

*Present address: Department of the Navy, Office of Naval Research, Branch Office, Box 39, FPO, New York 09510, USA.

0022–2461/84 $03.00 + .12

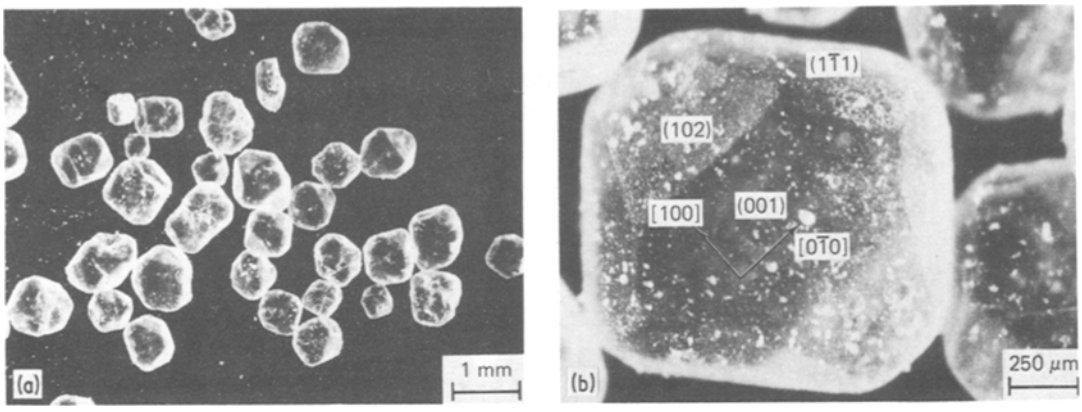

Figure 1 (a) Holston production-grade Class D RDX (cyclotrimethylenetrinitramine) crystals. (b) Identification of (0 0 1), (1 0 2), and (1 $\bar{1}$ 1) facets together with the [1 0 0] and [0 $\bar{1}$ 0] directions on the (0 0 1) facet for an individual Class D crystal exhibiting a tabular morphology.

indentations were employed to obtain exploratory information on the degree of plastic anisotropy for this orthorhombic crystal structure type. Vickers impressions were used to assess the spatial variation of hardness. For comparison, hardness measurements were made on the starting material: production-grade Class D RDX crystals usually having linear dimensions less than 1 mm on any crystal face.

The laboratory-grown crystals were crystallographically characterized using back-reflection and transmission Laue X-ray diffraction techniques. The crystal growth faces and their directions of intersection were identified. The morphologies are compared to RDX crystals of various polygonal shapes and sizes described in previous investigations [8–10].

In addition to the need for RDX crystal morphology information to perform controlled deformation and fracture studies [6, 11], the faceted morphologies of molecular (explosive) crystals are considered to be related to the internal structural perfection of the crystals [12, 13] and, hence, to their structure-sensitive properties [14, 15]. Consequently, specification of the crystal morphologies is also basic to obtaining a better understanding of crystal growth processes for these structures.

2. Crystal growth

The starting material was Holston production-grade Class D RDX crystals (see Fig. 1) chemically manufactured[16] by the nitration of hexamethylenetetramine. The Class D crystals were crystallized during processing from cyclohexanone and have a tabular habit; certain prominent planes and directions for the Class D product are marked in Fig. 1b according to a previous identification reported by Connick and May [10]. The identified crystal morphology was confirmed by using a method of optical trace analysis to be described later for the the faceted morphologies of the newly-grown crystals.

Numerous crystals of RDX of a few millimetres in size were grown by evaporation from Class D crystal stock put into solution in acetone. After preparing a concentrated solution of the RDX in reagent-grade acetone, the solution was allowed to evaporate completely in clean glass beakers without introducing seed crystals. By lightly covering the beakers with aluminium foil, "slow" grown crystals were obtained for comparison with "fast" grown crystals obtained from beakers left uncovered.

The resultant RDX crystals had two markedly different morphologies as shown in Figs. 2a and b. Many of the crystals (Fig. 2a) exhibited a prismatic morphology (I) resembling that shown by Connick and May [10] for crystals grown from solution in acetone. The crystals exhibited ± (0 1 0) facets on either side of the [0 0 1] prism axis with the longest dimension usually being parallel to the [0 0 1], as identified from the analysis of Laue experiments to be discussed. A second morphology (II) was found (Fig. 2b) having ± (0 0 1) facets on either side of the [0 1 0] axis with the longest dimension usually being parallel to [0 1 0]. An initial discussion of morphology II and microhardness measurements for it have been given [6]. Morphology II was also prismatic, although not as

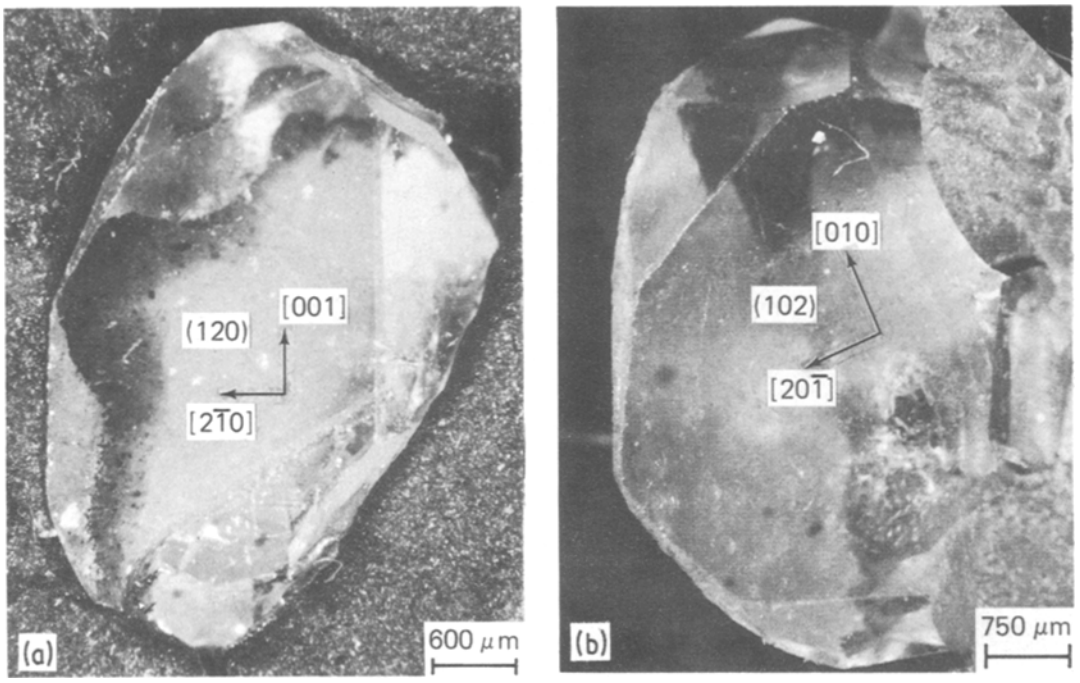

Figure 2 (a) Prismatic RDX crystal morphology (I) grown from solution in acetone and exhibiting a [0 0 1] prism axis with major (1 2 0) and ($\bar{1}$ 2 0) facets on either side of the exposed (0 1 0) face. (b) Prismatic RDX crystal morphology (II) grown from solution in acetone and exhibiting a [0 1 0] prism axis with major (1 0 2) and ($\bar{1}$ 0 2) facets on either side of the exposed (0 0 1) face.

readily identifiable as such. Both morphologies were observed for the "slow" and "fast" evaporation rates. Normally, the width of the (0 1 0) and (0 0 1) facets was diminished significantly for those crystals grown by "fast" evaporation. Larger crystals resulted when grown from the slower evaporating solution; some of these were selected for the X-ray orientation and hardness experiments to be described.

3. Chemical analysis

Since HMX (cyclotetramethylenetetranitramine) is formed [16] as a reaction by-product during the manufacture of RDX by nitrating hexamethylenetetramine, both Class D and various laboratory-grown RDX crystals were carefully analysed for HMX/RDX content using high performance liquid chromatography [17]. Analyses were performed on a Hewlett Packard Model 1084 chromatograph with a Model 1030 variable wavelength detector. Instrument operating conditions were: eluent, 2 ml min^{-1}; 30% methanol/water; attenuation 2^7 for HMX and 2^{10} for RDX; wavelength 254 nm. Analyses were made by comparing the peak heights that resulted from 25 μl injections of sample/methanol solutions with the peak heights obtained for 25 μl injections of a standard HMX/RDX/methanol solution (HMX = 0.216×10^{-3} M; RDX = 3.469×10^{-3} M). The HMX and RDX materials used to make the standard solution were recrystallized three times from acetone and dried. Their purity was verified by thin layer chromatography as well as by other chromatographic techniques.

A compilation of the analyses performed on crystals representative of those used in this work appears in Table I. The values that are reported are averages from at least three determinations, each one of which is expected to be accurate to ± 3%. Separate analyses were performed on morphology I and II crystals grown at the "fast" and "slow" evaporation rates, but the results for each crystal growth rate were indistinguishable. The laboratory-grown RDX crystals obtained at either rate had considerably lower HMX content than the as-received Class D crystals. Laboratory crystals grown at the slower evaporation rate were purer since crystallization was more controlled. Combining the amounts of HMX and RDX found from each of the first three analyses appearing in Table I indicated that unidentified constituents must account for between 1.3 and 3.8 wt %. Since

TABLE I Chemical analysis of RDX crystals

Designation	Wt % found		Total wt %
	HMX	RDX	
Class D, as-received	6.66	91.4	98.1
Laboratory-grown, "fast" evaporation	0.40	95.8	96.2
Laboratory-grown, "slow" evaporation	0.12	98.6	98.7
Class D, hand-picked	0.29	101	101
Class D, hand-picked and washed	0.17	98.4	98.6

no pronounced high molecular weight peaks were observed in the chromatograms, the most probable candidate is occluded solvent (cyclohexanone and acetone in the production-grade and laboratory-grown crystals, respectively). The presence of liquid inclusions in RDX has been reported by Gross [18] from optical microscopy results.

To determine whether the HMX found in the as-received Class D crystals primarily is accommodated in the RDX crystal lattice or crystallizes separately, two additional analyses were performed on hand-picked crystals that clearly had the tabular morphology of the RDX crystal appearing in Fig. 1b. One of these analyses was performed after the crystals had been washed three times in methanol to remove the fine dust (Fig. 1a) normally associated with the production-grade material. From these analyses, it was found that the HMX and other impurity contents were highly comparable in both the production-grade and laboratory-grown crystals. Almost all of the HMX found in the as-received Class D product apparently exists as separate crystals, and this would explain why a few of the Class D crystals did not seem to have the expected tabular morphology shown in Fig. 1b. Washing the sample before analysis somewhat lowered the HMX content indicating that the fine dust may contain HMX or that some HMX may be on the surface of the RDX crystals. For the present work, it is important to note that the RDX crystals described by Connick and May [10] were grown from RDX manufactured by the Woolwich Process which does not yield any HMX as a by-product.

4. Laue diffraction experiments

A Laue back-reflection photograph of the largest visible facet of the crystal in Fig. 2a, rotated 90° clockwise about the facet normal, is given in

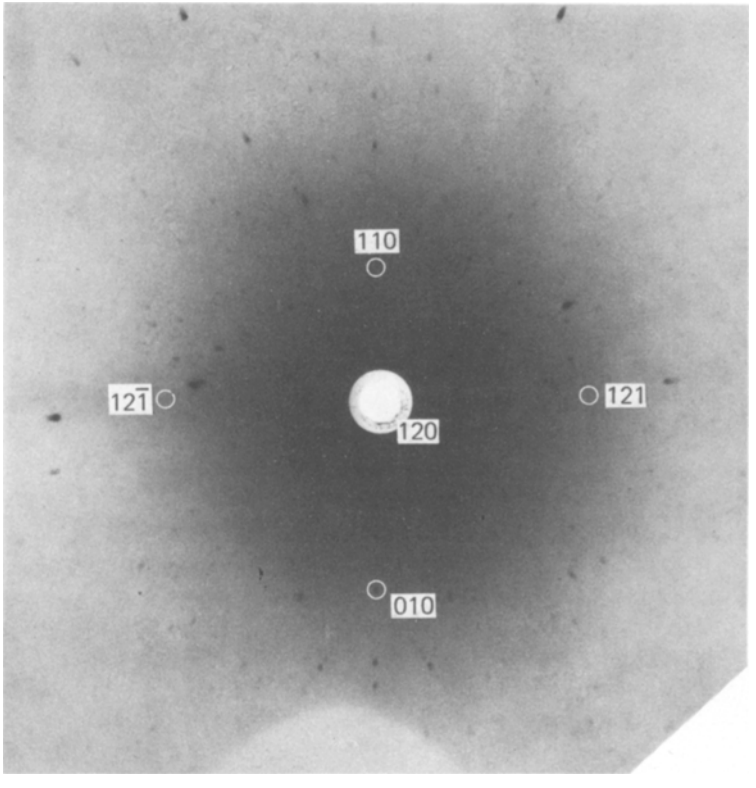

Figure 3 Laue back-reflection photograph on Ilford Industrial G film of RDX prismatic crystal morphology I obtained at 3 cm distance with a copper target operated for 3 h at 20 kV and 18 mA.

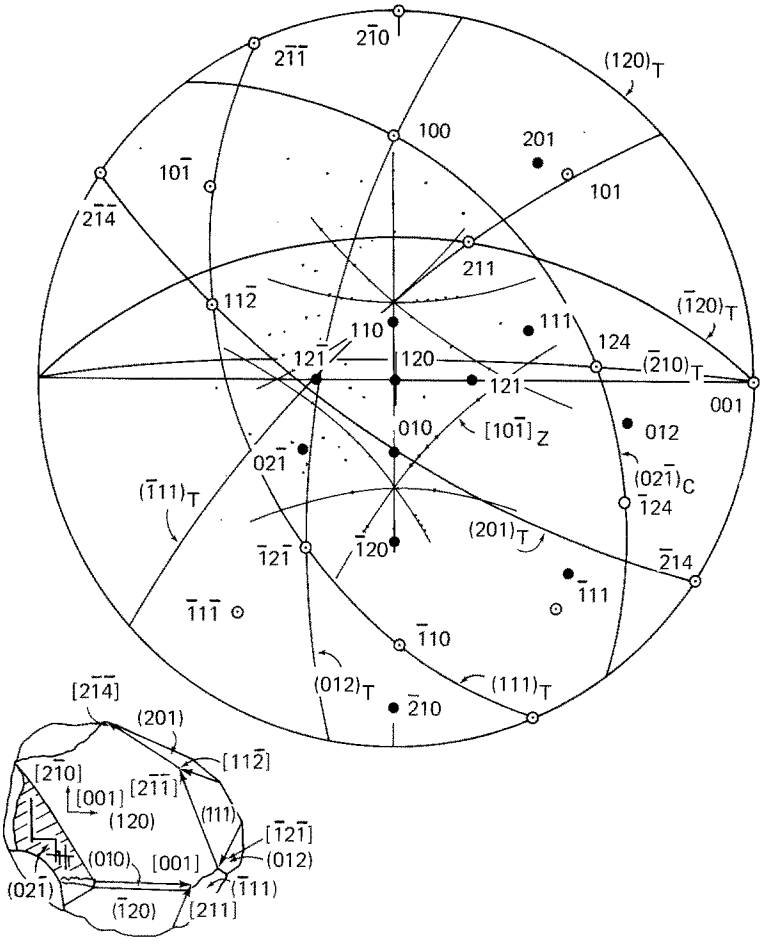

Figure 4 Stereographic projection of plane normals •, and directions ⊙, for RDX prismatic crystal morphology I, including the recorded Laue back-reflection spots and matching the visual crystal appearance which is also shown schematically.

Fig. 3. The facet is a (1 2 0) surface. The pattern was obtained using a copper tube on a conventional spot focus Phillips X-ray generating unit operated at 20 kV and 18 mA for 3 h with a Griak back-reflection camera and standard collimator. The photograph was recorded with Ilford Industrial G film at a 3 cm distance. No particular fluorescence problem occurred under these conditions as compared with initial attempts with a different RDX crystal using a molybdenum tube operated first at 35 kV and 15 mA for 1.5 h and then also at 30 kV and 20 mA for 1.5 h even with aluminium foil employed as a filter. Fig. 4 shows the stereographic projection used to analyse the X-ray diffraction pattern according to the standard method [19] of plotting zone directions and identifying them by comparison with calculated angles between directions. The angles between the directions and planes of the orthorhombic *Pbca* space group for RDX were computed by taking $a = 1.3182$ nm, $b = 1.1574$ nm, and $c = 1.0709$ nm [20]. For direct reference to the physical appearance of the crystal, the (tiny) spots of the diffraction pattern and an appropriately labelled schematic view of the crystal (in the lower left corner) are shown together with the stereographic analysis of Fig. 4 as viewed from the position of the X-ray source. The (1 2 0) stereographic projection appearing in Fig. 5 was prepared to give a reference view of the crystal symmetry associated with the specific (rotated) orientation of the crystal appearing in Fig. 2a.

By matching the alignment of the various edges of plane interactions shown for the crystal features in Fig. 2a with the identified crystallographic planes and directions in Fig. 5, a reasonably complete determination was made of the total crystal morphology, appearing schematically in Fig. 4. For example, the specific [0 0 1], $[2\,\bar{1}\,\bar{1}]$, and $[2\,\bar{1}\,\bar{4}]$ directions were readily identified in Fig. 4 by diametral traces intersecting the circumferential circle representing the (1 2 0) surface. Since these directions should be produced by the intersection of the (1 2 0) plane with the (0 1 0), (1 1 1), and

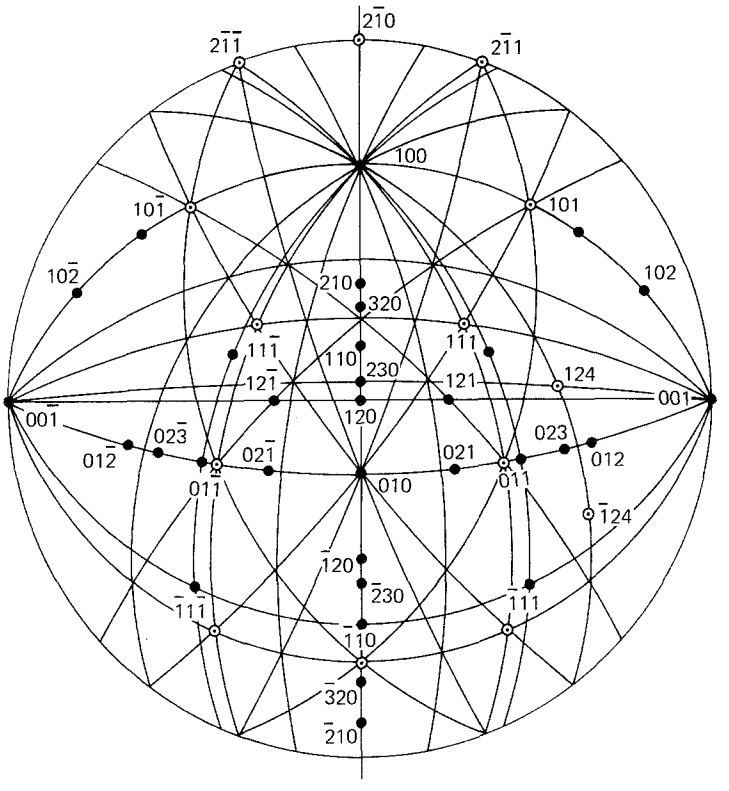

Figure 5 Standard (1 2 0) projection with indices marked for plane normals •, and direction ⊙.

(2 0 1) planes, respectively, relating to previous results [8–10, 12] reported for RDX crystal morphologies, such tentative indices were initially determined as acceptable ones for the specific planes in each particular case. The choice of planes was then either confirmed or corrected according to the measurement of the traces of additional directions of plane intersections which were observed for adjacent crystal faces other than the (1 2 0) facet. Determination of the indices for these directions was also accomplished, by projecting them radially onto the (1 2 0) surface. In addition to measurements of this type for the natural growth faces, the orientation of a prominent cleavage surface intersecting the (1 2 0) growth surface was identified in Fig. 4 as being (0 2 $\bar{1}$). Striations on this surface are clearly visible in the higher magnification view in Fig. 6. Interestingly, the (0 2 $\bar{1}$) does not appear to have been previously identified as a cleavage-type plane.

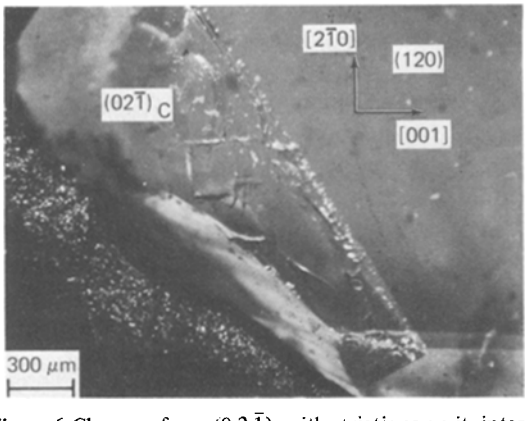

Figure 6 Cleavage face, (0 2 $\bar{1}$), with striations on it, intersecting the (1 2 0) growth facet of crystal morphology I (see Fig. 4).

Considering now the RDX crystal in Fig. 2b representing the new morphology II, a Laue transmission photograph was taken through the (1 0 2) facet, and the result is shown in Fig. 7. The facet was determined to be (1 0 2) from the stereographic projection analysis given in Fig. 8 of the combined diffraction pattern and crystal morphology, again both viewed with directions and plane normals emanating from the (1 0 2) crystal surface. The diffraction pattern in Fig. 7 was obtained for the same operating conditions detailed for the back-reflection photograph in Fig. 3, except that the exposure time was reduced from 3 to 2.5 h. The crystal thickness was approximately 3 mm. In Fig. 8, the zone axes of the two most prominent ellipses were found to be [2 0 3] and [0 0 1] as indicated near the centre of the

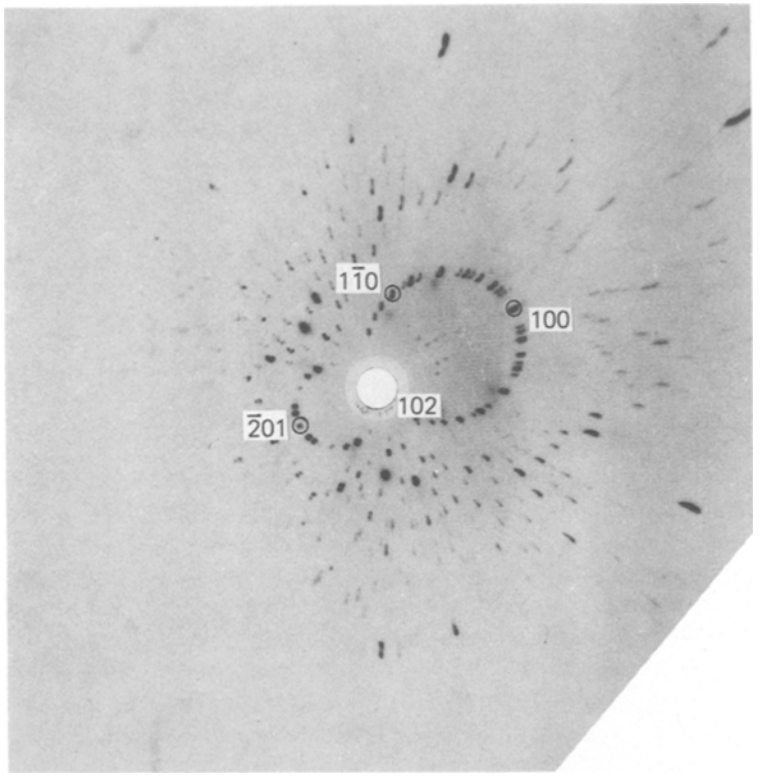

Figure 7 Laue transmission photograph on Ilford Industrial G film of 3 mm thick RDX crystal morphology II obtained at 3 cm distance with a copper target operated for 2.5 h at 20 kV and 18 mA.

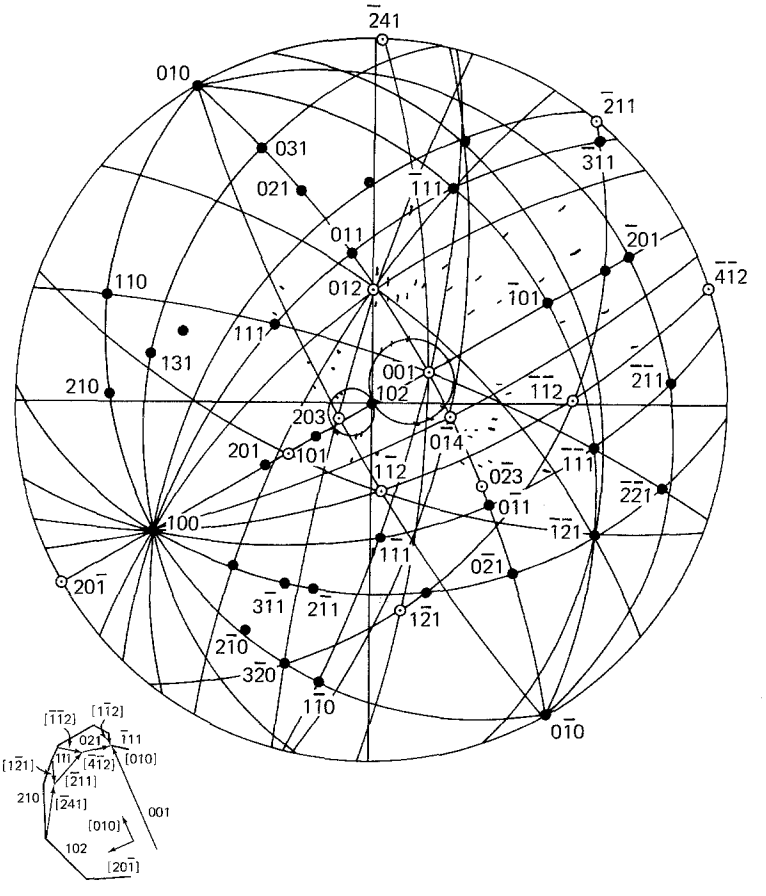

Figure 8 Stereographic projection of plane normals •, and directions ⊙, for RDX crystal morphology II, including the recorded Laue transmission spots and matching the visual crystal appearance which is also shown schematically (see Fig. 2b).

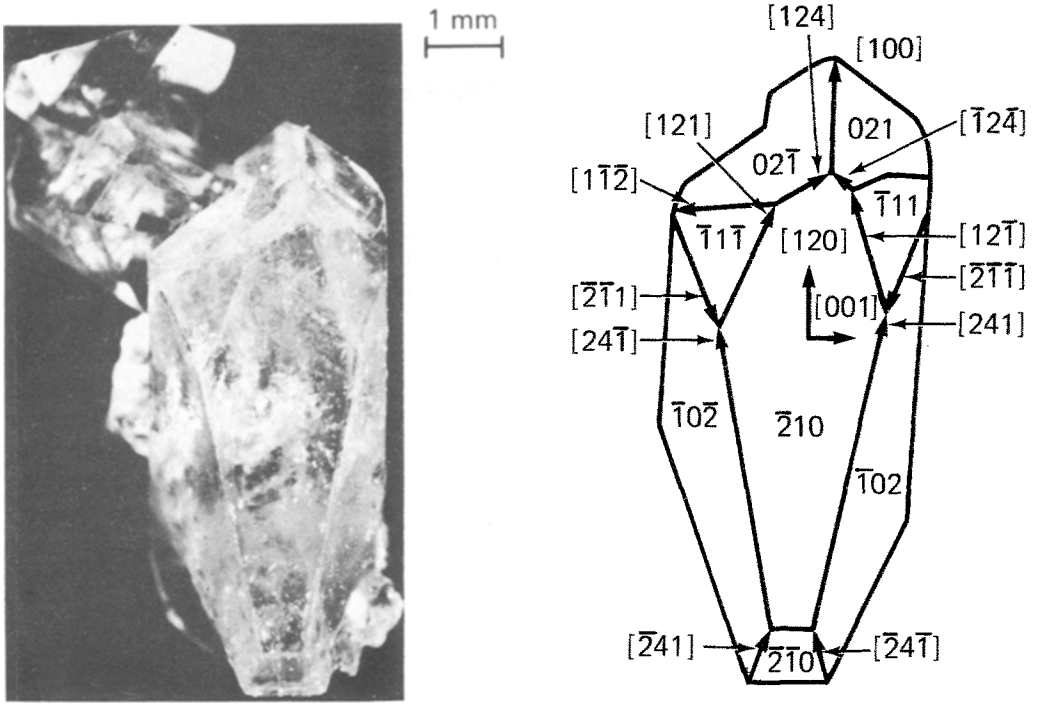

Figure 9 RDX crystal morphology II with exposed growth faces and directions identified on a schematic drawing.

projection. Since so few zones were easily recognizable in the transmission photograph, a conclusive orientation analysis depended primarily on the determination of a large number of specific low index plane poles appearing in the stereographic projection. An optical trace analysis, as described previously, allowed specification of the other recognizable facets and the directions of their intersections.

A back-reflection Laue experiment was previously described [6] for a second crystal (Fig. 9) having morphology II with a large $(\bar{2}\,1\,0)$ growth

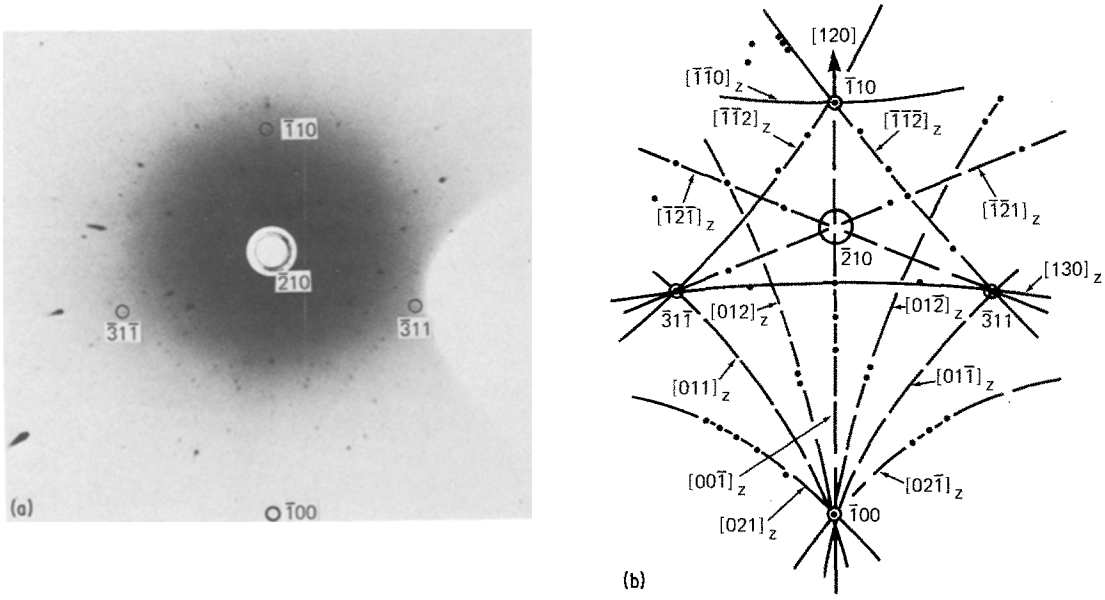

Figure 10 (a) Laue back-reflection photograph on Ilford Industrial G film of RDX crystal morphology II, obtained at 3 cm distance with a copper target operated for 1.5 h at 25 kV and 12.5 mA. (b) Zone (and plane pole) analysis of Laue back-reflection pattern to identify the $(\bar{2}\,1\,0)$ crystal surface as directly viewed.

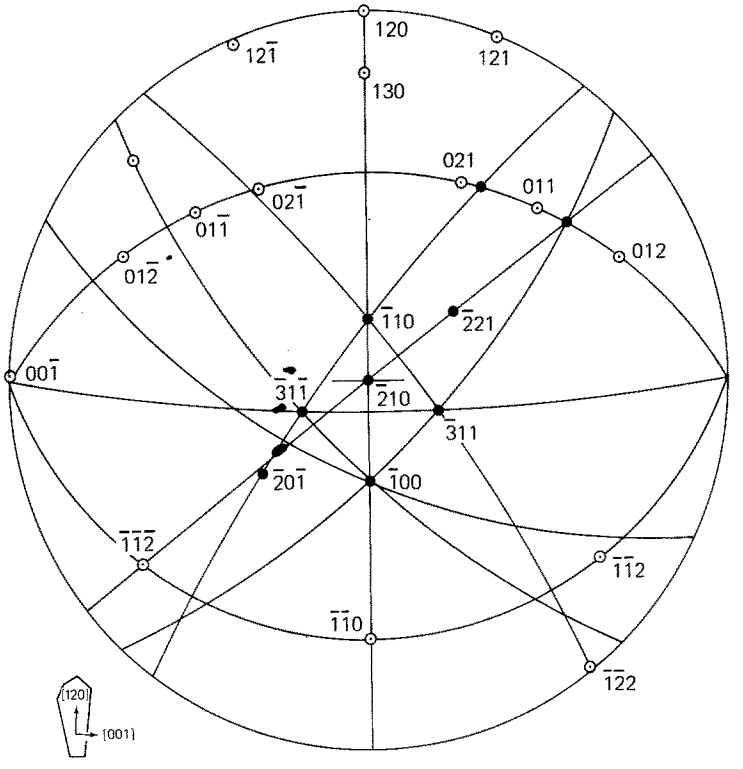

Figure 11 Stereographic projection analysis for zone directions and plane poles obtained in Laue back-reflection pattern of $(\bar{2}\,1\,0)$ surface exposed in crystal morphology II.

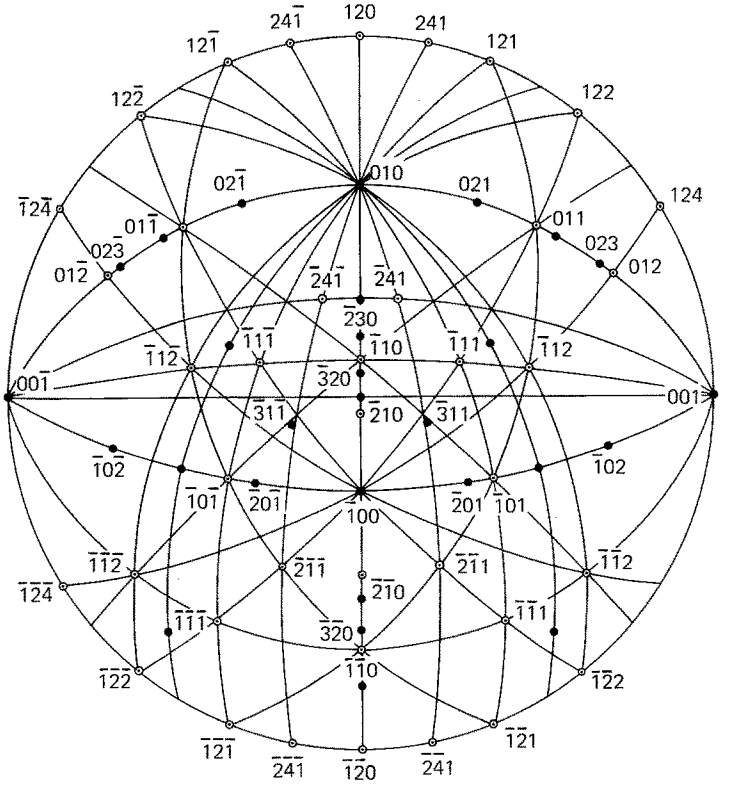

Figure 12 Standard $(\bar{2}\,1\,0)$ projection with indices marked for plane normals •, and directions ⊙.

face. A more complete analysis and description of this result is now reported. The Laue photograph of the $(\bar{2}\,1\,0)$ facet appears in Fig. 10a along with the traced diffraction pattern in Fig. 10b, identifying a number of zones and a few plane poles. It is important to note that the described view for Fig. 10 of the crystal in Fig. 9 is nearly orthogonal to the view of the crystal in Fig. 2b where the (2 1 0) facet is observed at the left edge of the crystal (Fig. 8 also). The stereographic projection in Fig. 11 was employed for the full determination of the crystallographic features in Fig. 9. The results may be compared with the $(\bar{2}\,1\,0)$ stereographic projection for selected plane normals and directions shown in Fig. 12.

5. Microhardness experiments

Using a Tukon microhardness tester (Model FB), some room temperature deformation experiments were performed on three laboratory-grown crystals and on a few production-grade Class D RDX crystals. The most extensive testing was performed on the $(\bar{2}\,1\,0)$ growth face of the unmounted crystal having morphology II appearing in Fig. 9 [6]. Hardness measurements on this crystal in a free-standing condition were possible because the top and bottom surfaces were found to be highly parallel. Vickers measurements were made to determine the spatial variation of hardness, while the long axis of the Knoop indenter was aligned along several crystallographic directions to assess plastic anisotropy. Knoop hardness measurements were also made on two mounted crystals having morphology I, including the crystal shown in Fig. 2a. For these two crystals, a preliminary assessment of plastic anisotropy was also determined. These results are summarized in Table II together with the hardness measurements reported previously for the morphology II crystal [6]. All of the measurements on the laboratory-grown crystals were made at a 50 g load.

A few Knoop hardness measurements at 50 g load were made on the (0 0 1) growth face of two unmounted production-grade Class D RDX crystals and are given in Table III. In addition Vickers measurements were attempted at 50 g load, initially on a series of these crystals with one pyramid diagonal aligned in several different directions in the (0 0 1) surface. The crystals used in the Vickers experiments were held by double-sided tape. This results in the measured hardness values being a little lower than the actual values. Some measurements were made at 100 g load to allow better resolution of the crystallographically-determined crack traces that emerged in the (0 0 1) surface. Vickers hardness measurements made on two crystals at 100 g load, with one pyramid diagonal being roughly parallel (within 10 to 11.5°) to [1 1 0], are included in Table III. Aligning the pyramid diagonal considerably off [1 1 0] yielded badly distorted impressions that were not suitable for hardness measurements. However, varying the indenter diagonal alignment did not substantially alter the crystallographic alignment of the cracking pattern.

6. Discussion

Morphology I of the RDX crystals grown in this work is somewhat similar to that analysed by Connick and May [10] from interfacial angle

TABLE II Summary of hardness values obtained for various growth faces of laboratory-grown RDX crystals (50 g load)

Crystal morphology	Growth face	Indenter	Hardness (N mm^{-2})	Orientation of indenter axis
I	(1 2 0)	Knoop	280; 280; 280; 300	[0 0 1]
		Knoop	230*; 310; 390; 420	[2 $\bar{1}$ 0]
I	(0 1 0)	Knoop	170; 230; 240	[0 0 1]
		Knoop	160†; 280; 310	[1 0 0]
II	$(\bar{2}\,1\,0)$	Knoop	290	[0 0 $\bar{1}$]
([6])		Knoop	310	[1 2 0]
		Knoop	420; 700	Perpendicular to [2 4 $\bar{1}$] (or near-parallel to [0 0 $\bar{1}$])
		Knoop	280; 280; 320	Parallel to [2 4 $\bar{1}$] (or near-parallel to [1 2 0])
		Vickers	310; 330; 350; 380	(Pyramid diagonal) parallel to [0 0 $\bar{1}$]

*Unusual cracking associated with this hardness impression.
†Very asymmetric impression.

TABLE III Summary of hardness values obtained for production-grade Class D RDX

Approximate crystal dimension (μm) (tabular morphology with (0 0 1) growth face)	Indenter	Hardness (N mm^{-2})	Observation
1100	Knoop (50 g load)	210; 250	Indenter axis 6° from [0 1 0]; sub-surface (0 0 1) cracking
800	Knoop (50 g load)	770	Indenter axis 9° from [0 1 0]; sub-surface (0 0 1) cracking
		430	Indenter axis 5° from [1 0 0]; sub-surface (0 0 1) cracking
1900	Vickers (100 g load)	290	Pyramid diagonal 10° from [1 1 0]; diagonal cracking along ± [$\bar{1}$ 1 0] radii and along radii perpendicular to ± (1 1 0); sub-surface (0 0 1) cracking
2200	Vickers (100 g load)	490	Pyramid diagonal 11.5° from [1 1 0]; diagonal cracking along ± [$\bar{1}$ 1 0] radii and along radii perpendicular to ± (1 1 0); sub-surface (0 0 1) cracking

measurements on crystals grown from acetone or, alternatively, from dimethylformamide solution. Fox and Levine [9] have also examined RDX crystals grown from acetone solution using optical goniometry, and their description differs in two important aspects from that given by Connick and May. First, the (0 0 1) facet of the Fox and Levine crystals has a larger area than either the (1 0 0) or (0 1 0), while Connick and May show (on the basis of the identification of the unit cell area given by Reed [21]) the (0 1 0) face as the largest of these three facets. Second, Fox and Levine identify eight small {3 6 4} faces that are absent both in the crystals described by Connick and May and in the crystals characterized in this work. The morphology II crystals obtained in this work are unique compared to morphology I crystals due to the combined existence of prominent (0 0 1) and (2 1 0) growth faces. As expected from the difference in prismatic as opposed to tabular growth forms obtained by Connick and May for RDX crystallized from acetone and cyclohexanone solution, respectively, the morphologies of the laboratory-grown crystals did not resemble the Class D production-grade crystals. Nor did the crystals grown in this work resemble the tabular from of RDX illustrated by McCrone [8].

Some portions of the crystals grown in this work were not perfectly transparent. Such optical dispersion indicates the presence of internal imperfections or strain centres. This was substantiated by the unusual streaking or asterism of some of the Laue diffraction spots.

The strikingly different intensities of certain sets of individual diffraction spots in both the back-reflection and transmission diffraction patterns seem to be somewhat anomalous. This is so despite the well-known lack of correlation expected for the reflected intensities of all the diffracted spots in such patterns, due to the polychromatic radiation used to obtain the patterns and the differences in the degree of superposition of multiple order reflections at the individual reflected beam positions [22]. In general, it was not possible to identify individual spots within such prominent sets as being reasonably low index reflections on the basis of the structure factors previously specified for RDX [12, 21]. This suggests the possibility that such plane reflections are associated with the accommodation of some impurity, most probably acetone, in the host lattice, resulting in a changed extinction property for these planes because of the changed atomic or molecular positions and consequent lattice strains.

The physical appearance of the RDX crystals was not visibly altered by the individual X-ray exposures nor was any deterioration observed in obtaining repeated diffraction patterns. However, considerable difficulty has been experienced in initial attempts to obtain Berg–Barrett topographs of these crystals. This indicates that the perfection of the laboratory-grown crystals is probably not adequate to obtain X-ray topographs easily. To some extent, this difficulty with the internal perfection of molecular crystals of this complexity is responsible for the concerted effort of other investigators [23] to produce exceptionally perfect crystals, including RDX [12, 24], and to examine

carefully their dislocation contents with the extremely sensitive technique of Lang topography. In such experiments, the strain fields of individual dislocations have been observed to extend over distances of the order of hundreds of microns, in agreement with the calculation of the extinction distance for X-rays [12]. This compares with tens of microns for these distances in metallic, ionic, and covalent crystals [25, 26].

The hardness values obtained for the various laboratory-grown RDX crystals compare favourably with the values measured for the individual Class D crystals. However, a strict comparison should not be made because different growth surfaces have been indented in each case as a consequence of the difference in prismatic as opposed to tabular crystal morphologies. A Vickers hardness of 236 $N mm^{-2}$ has been reported by Hagan and Chaudhri [11] for RDX, and this value is somewhat lower than the Vickers hardnesses given in Tables II and III. Although a lower hardness might be indicative of softer, more perfect crystals, there is the greater possibility that the lower hardness was obtained because of an increased amount of cracking being associated with this previously reported hardness value. In earlier work, Bowers *et al.* [27] report a Vickers hardness of about 340 $N mm^{-2}$ for RDX that more closely agrees with the values obtained in this work.

A significant feature of the hardness results in Tables II and III is the observation that the spatial variation of the Vickers or Knoop hardnesses for a given surface is comparable to, or in several instances larger than, the hardness anisotropy measured for the various orientations of the Knoop indentations on a single surface. One reason for this is that both the laboratory-grown and particularly the Class D RDX crystals contain inclusions and pores which, in some instances, are roughly the same size as the hardness impressions themselves. The internal structures and stresses of these nearly macroscopic defects can be observed visually and, at least in part, these defects determine the degree to which the various crystals are optically transparent. These large-scale defects should act as obstacles to the progression of slip (or twinning) and even cleavage cracking mechanisms within the otherwise perfect RDX crystal lattice. Thus, it is important to investigate the mechanical behaviour of real crystals with such defects. A second reason for the spatial variation in hardness is related to the crystal growth process which generally occurs by the cooperative development of individual growth sectors [13] comprising the entire crystal mass. The Burgers and line vectors of the relatively few dislocations observed in even the most carefully grown crystals reported on to date differ according to the nature of the growth sectors containing them [13, 24].

Using light microscopy, it was difficult to observe any clear definition of slip plane or slip band traces at the hardness impressions, despite repeated attempts to do so at all types of indentations. This difficulty is attributed in part to the obscuring effect of the large-scale internal defects, but is ascribed primarily to the extreme localization of the deformational zones [6] surrounding the hardness indentations. An unlikely contributing factor is the relatively high homologous temperature (T/T_M is 0.625, where the melting temperature (T_M) for RDX is 204° C) at which the hardness testing has been performed in that appreciable dislocation climb or cross-slip could be occurring. The most likely reason for the absence of well-defined slip observations is probably due to the fundamental difficulty of generating dislocations and moving them within the molecular structure of RDX.

The particular difficulty of observing directly any slip band structure has led to investigating the usefulness of model structural considerations, taken from the orthorhombic unit cell [6] depicted in Fig. 13, for determining information about the expected deformation behaviour of RDX. The figure has been constructed according to the structural work of Reed [21] and more recently of Choi and Prince [20]. The observation [10, 12] that (0 0 1) cleavage is favoured compared to (1 0 0) or (0 1 0) cleavage seems understandable based on the intermolecular distances between the molecules in the unit cell. A significant observation from dislocation etch pit studies by Connick and May [10] and from X-ray topography results obtained by McDermott and Phakey [12] is that dislocations have been assigned to have the largest Burgers vector of $\mathbf{b} = a[1\,0\,0]$ among the three orthogonal unit vectors for the cell structure. Self-energies for the unit vector dislocations taken proportional to b^2 of 1.147, 1.340, and 1.738 nm^2 are expected on this basis for the $c[0\,0\,1]$, $b[0\,1\,0]$, and $a[1\,0\,0]$ dislocations, respectively. A greater energy involved in forming the largest unit vector dislocation would be scaled accordingly. A relatively large anisotropy in shear modulus would be

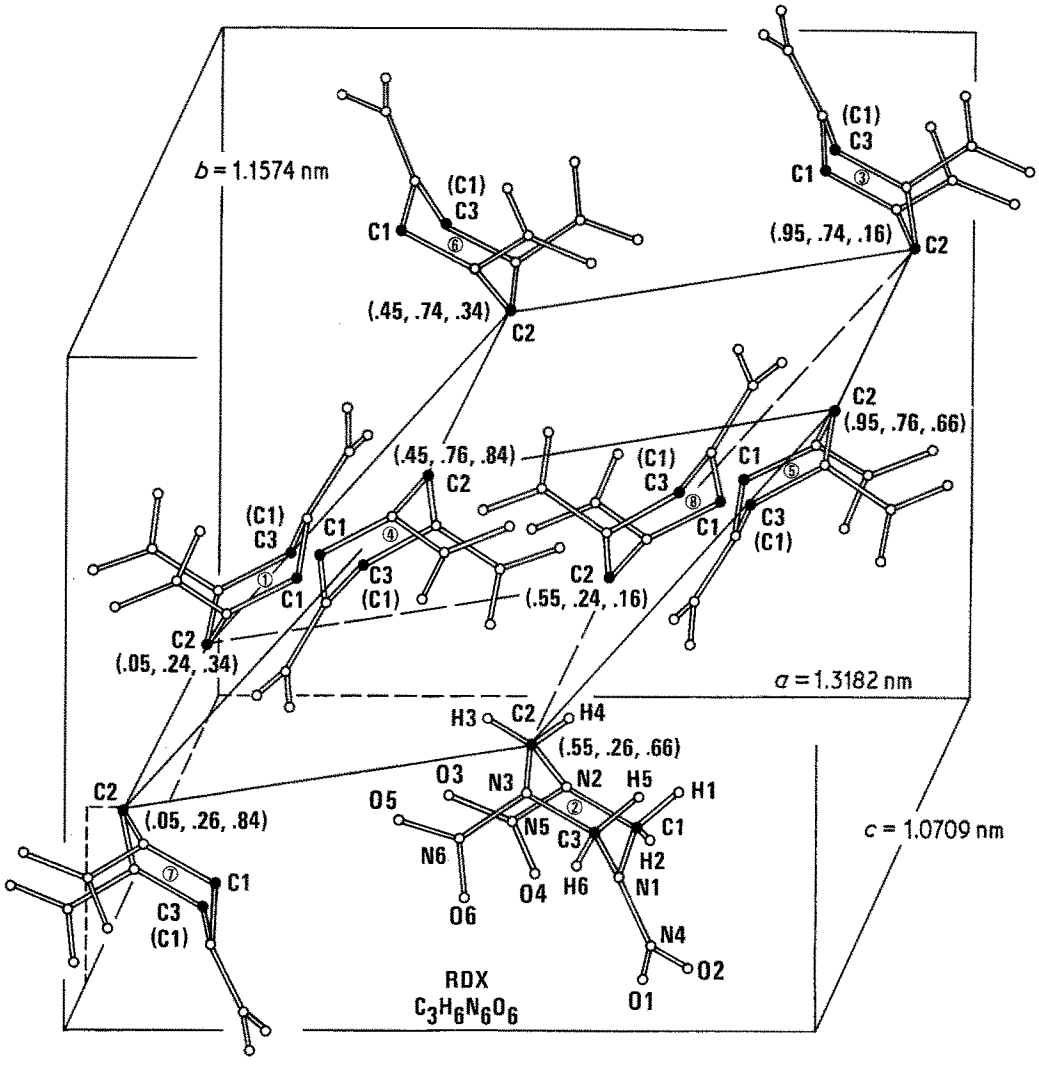

Figure 13 Orthorhombic unit cell for RDX: cyclotrimethylenetrinitramine.

necessary to change the energy hierarchy obtained on this basis. Complete elastic constant data are not available generally for explosive molecular crystals; however, elastic wave propagation data reported by Morris [28] for PETN (pentaerythritol-tetranitrate) reveal the shear modulus to be fairly isotropic [about 25% variation between (1 0 0) or (0 1 0) and (1 1 0)].

The consideration arises from the unit cell that the $a[1\,0\,0]$ dislocation would require on (0 1 0) or (0 2 1), for example, the interleaving of four planes of $(h\,0\,0)$ type. This suggests the possibility that the $a[1\,0\,0]$ dislocation might favourably decompose into partial dislocations. In fact, using the (0 2 1) as an example, the reaction

$$[\bar{1}\,0\,0] \rightarrow \tfrac{1}{6}[\bar{2}\,\bar{1}\,2] + \tfrac{1}{6}[\bar{1}\,0\,0] + \tfrac{1}{6}[\bar{2}\,1\,\bar{2}] + \tfrac{1}{6}[\bar{1}\,0\,0]$$

seems a favourable possibility of giving

$$\sum_{p=1}^{4} b_p^2 = 0.81\ \text{nm}^2$$

without regard for the energies of stacking faults between the partial dislocations, and thus seems to be a worthwhile consideration for understanding the occurrence of $a[1\,0\,0]$ dislocations. Further study is needed of this type of model consideration for understanding the total deformation properties of RDX, particularly with regard to elucidating the nature of initiation of its chemical decomposition.

7. Conclusions

1. Well-established back-reflection and transmission Laue results have been obtained for specifiying the variable crystal morphologies of

laboratory RDX crystals having HMX and other impurity contents comparable to production-grade Class D RDX used as the starting material. The X-ray diffraction results were confirmed by an analysis of optical measurements. The combined results were described on a stereographic projection basis.

2. Initial hardness results from measurements on these RDX crystals and on production-grade crystals revealed a very significant plastic anisotropy, despite the lack of definition of specific slip systems. The large plastic anisotropy is indicative of few slip systems being operative and, hence, is one reason for the observation, in a previous dislocation etch-pit study [6], that the plastic deformation is highly localized at the hardness impressions is such laboratory-grown crystals. Considerable spatial inhomogeneity was also observed indicating the presence of internal obstacles.

3. An encouraging preliminary analysis has been made of the deformation and cleavage properties of RDX by considering its unit cell structure. In particular, the previous observation of a[1 0 0]-type dislocations has been attributed to partial dislocations giving a low energy for the otherwise large Burgers vector dislocation.

Acknowledgements

This work was supported partially by the Independent Research Program (Work Unit IR-561) at the Naval Surface Weapons Center (NSWC) and partially by the Office of Naval Research under work request number N0001482WR20129. The authors wish to express their appreciation to Dr R. R. Bernecker for his encouragement and helpful comments. The Laue experiments were performed in the NSWC laboratory of Drs J. R. Holden and C. W. Dickinson with their help and advice. The authors gratefully acknowledge the many useful discussions on the crystal structure of RDX held with Drs J. M. Stewart (University of Maryland), E. Prince (National Bureau of Standards, Washington, DC) and J. R. Holden.

References

1. F. P. BOWDEN and A. D. YOFFE, "Fast Reactions in Solids" (Butterworths Scientific Publications, London, 1958).
2. S. J. JACOBS, T. P. LIDDIARD and B. E. DRIMMER, in Ninth Symposium (International) on Combustion, Ithaca, New York, August 27–September 1, 1962 (Academic Press, New York and London, 1963) p. 517.
3. H. S. NAPADENSKY, in Behavior and Utilization of Explosives in Engineering Design, Albuquerque, NM, March 1972 (New Mexico Section ASME, 1972) p. 57.
4. A. W. CAMPBELL, M. E. MALIN and T. E. HOLLAND, in Second ONR Symposium on Detonation, Washington, DC, and White Oak, MD, February 1955 (Office of Naval Research, Department of the Navy, Washington, DC, 1955) p. 336.
5. G. K. ADAMS, J. HOLDEN and E. G. WHITBREAD, in Extrait du Compte-rendu du XXXI Congrès International de Chimie Industrielle dans la Section Poudres et Explosifs, Liège, September 1958 [*Ind. Chim. Belge Suppl.* **2** (1959) 216] p. 1.
6. W. L. ELBAN and R. W. ARMSTRONG, in Proceedings of the Seventh Symposium (International) on Detonation, Annapolis, MD, 16–19 June 1981 (Naval Surface Weapons Centre, Silver Spring, MD, 1982, NSWC MP 82-334) p. 976.
7. R. W. ARMSTRONG, C. S. COFFEY and W. L. ELBAN, *Acta Metall.* **30** (1982) 2111.
8. W. C. McCRONE, *Anal. Chem.* **22** (1950) 954.
9. H. W. FOX and O. LEVINE, "The Wettability of RDX and PETN Crystal Surfaces", NRL Report 4714 (1956).
10. W. CONNICK and F. G. J. MAY, *J. Cryst. Growth* **5** (1969) 65.
11. J. T. HAGAN and M. M. CHAUDHRI, *J. Mater. Sci.* **12** (1977) 1055.
12. I. T. McDERMOTT and P. P. PHAKEY, *Phys. Status Solidi (a)* **8** (1971) 505.
13. H. KLAPPER, in "Characterization of Crystal Growth Defects by X-Ray Methods", edited by B. K. Tanner and D. K. Bowen (Plenum Press, New York, 1980) p. 133.
14. J. diPERSIO and B. ESCAIG, *Phys. Status Solidi (a)* **40** (1977) 393.
15. J. N. SHERWOOD, in "The Plastically Crystalline State-Orientationally Disordered Crystals", edited by J. N. Sherwood (Wiley and Sons, New York, 1979) p. 39.
16. T. URBAŃSKI, "Chemistry and Technology of Explosives", Vol. III, First English Edition (Pergamon Press, Oxford, 1967) pp. 87–98.
17. J. C. HOFFSOMMER, D. A. KUBOSE and D. J. GLOVER, "Microanalysis of Selected Energetic Nitro Compounds by Gas/Liquid Chromatography" (GC/LC), NSWC TR 80-535 (1981).
18. K. A. GROSS, *J. Cryst. Growth* **6** (1970) 210.
19. C. S. BARRETT and T. B. MASSALSKI, "Structure of Metals" 3rd edn (McGraw-Hill, New York, 1966) pp. 211–18.
20. C. S. CHOI and E. PRINCE, *Acta Crystallogr.* **B28** (1972) 2857.
21. P. T. REED, in "Structures of Trinitro-Aromatic Crystals and Related Substances", edited by P. M. Harris, AFOSR-TR-59-165 (1959) p. 6.
22. C. S. BARRETT and T. B. MASSALSKI, "Structure of Metals" 3rd edn (McGraw-Hill, New York, 1966) pp. 171–92.
23. J. BLEAY, R. M. HOOPER, R. S. NARANG and J. N. SHERWOOD. *J. Cryst. Growth* **43** (1978) 589.

24. J. N. SHERWOOD, Private communication (1982).
25. R. W. ARMSTRONG and C. Cm. WU, in "Microstructural Analysis: Tools and Techniques", edited by J. L. McCall and W. M. Mueller (Plenum Press, New York and London, 1973) p. 169.
26. R. W. ARMSTRONG, in "Characterization of Crystal Growth Defects by X-Ray Methods", edited by B. K. Tanner and D. K. Bowen (Plenum Press, New York and London, 1980) p. 349.
27. R. C. BOWERS, J. B. ROMANS and W. A. ZISMAN, "Mechanisms Involved in the Impact Sensitivity of RDX Explosive Compositions", NRL Report 5463 (1960).
28. C. E. MORRIS, in Sixth Symposium (International) on Detonation, Coronado, CA, August 1976 (Office of Naval Research, Department of the Navy, Arlington, VA, ACR-221) p. 396.

Received 8 November 1982
and accepted 15 June 1983